AIP | Applied Physics Letters

Coherency strain enhanced dielectric-temperature property of rare-earth doped BaTiO3

Sang-Chae Jeon and Suk-Joong L. Kang

Citation: Applied Physics Letters **102**, 112915 (2013); doi: 10.1063/1.4798273
View online: http://dx.doi.org/10.1063/1.4798273
View Table of Contents: http://scitation.aip.org/content/aip/journal/apl/102/11?ver=pdfcov
Published by the AIP Publishing

Articles you may be interested in

Electrical, magnetic, and magneto-electrical properties in quasi-two-dimensional K0.58RhO2 single crystals doped with rare-earth elements
Appl. Phys. Lett. **105**, 062408 (2014); 10.1063/1.4893324

Fiber-optic thermometer application of thermal radiation from rare-earth end-doped SiO2 fiber
Rev. Sci. Instrum. **85**, 084903 (2014); 10.1063/1.4893483

Enhanced dielectric properties of BaTiO3/poly(vinylidene fluoride) nanocomposites for energy storage applications
J. Appl. Phys. **113**, 034105 (2013); 10.1063/1.4776740

Enhanced microwave dielectric properties of Ba0.4Sr0.6TiO3 ceramics doping by metal Fe powders
J. Appl. Phys. **112**, 104104 (2012); 10.1063/1.4766276

Dielectric properties and relaxor behavior of rare-earth (La, Sm, Eu, Dy, Y) substituted barium zirconium titanate ceramics
J. Appl. Phys. **102**, 084106 (2007); 10.1063/1.2799081

Free online magazine
MULTIPHYSICS SIMULATION
READ NOW
COMSOL

This article is copyrighted as indicated in the article. Reuse of AIP content is subject to the terms at: http://scitation.aip.org/termsconditions. Downloaded to IP: 143.248.118.104 On: Thu, 11 Sep 2014 07:35:02

Coherency strain enhanced dielectric-temperature property of rare-earth doped $BaTiO_3$

Sang-Chae Jeon and Suk-Joong L. Kang[a)]
Materials Interface Laboratory, Department of Materials Science and Engineering, Korea Advanced Institute of Science and Technology, 373-1, Guseong-dong, Yuseong-gu, Daejeon 305-701, South Korea

(Received 8 January 2013; accepted 11 March 2013; published online 22 March 2013)

Core/shell-grained $BaTiO_3$ samples were prepared with addition of rare earth elements. The core/shell interface was semi-coherent, and many misfit dislocations formed in Dy-doped samples. In contrast, a coherent interface and few dislocations were observed in Ho- and Er-doped samples. Dy-doped samples exhibited poor temperature stability, showing a peak with no frequency dispersion. Ho- and Er-doped samples exhibited a broad curve with frequency dispersion. This improved temperature stability is attributed to the coherency strain, which leads to the formation of polar nano-regions in the shell. Coherency at the core/shell interface is critical to improve the temperature stability of core/shell-structured $BaTiO_3$. © *2013 American Institute of Physics*. [http://dx.doi.org/10.1063/1.4798273]

Stable dielectric-temperature behavior is required for application of $BaTiO_3$-based ceramics in multilayer ceramic capacitors (MLCCs). Since a report by Kahn,[1] the formation of a core/shell structure in $BaTiO_3$-based ceramics has attracted much attention from researchers because of its significant contribution to enhancing dielectric-temperature stability.[2–10] The enhanced stability has been attributed to chemical inhomogeneity[2,5,11] and stored internal stresses in grains.[3,12] The chemical inhomogeneity includes a compositional fluctuation in the shell region and a compositional difference between the core and the shell. The shell phase has a range of phase transition temperature, which can exhibit diffuse phase transition (DPT) behavior, showing temperature insensitive dielectric permittivity.[2,5,11] The internal stresses formed in core/shell grains were also suggested to have a significant effect on the dielectric-temperature behaviors of $BaTiO_3$.[3] The nonuniform substitution of Ba or Ti with other elements that have different ionic sizes also causes a continuous change in the lattice parameter and thus a lattice distortion in the shell region. Internal stresses can also be developed during cooling of the core/shell grains as a result of the discrepancy in the phase transition temperature between the core and the shell: the core phase of pure $BaTiO_3$ transforms from cubic to tetragonal at about 120 °C while the shell phase maintains a pseudo-cubic structure down to room temperature. A lattice strain arises mainly at the core/shell boundaries. For both thin film and bulk $BaTiO_3$ materials the internal stresses resulting from the residual strain can drastically change the phase transition behavior.[12–14]

For a given core/shell structure, however, it has been difficult to differentiate the aforementioned two contributions, chemical inhomogeneity and internal stresses. However, by preparing two kinds of samples with the same core/shell structures but with different residual strain states, it will be possible to observe the strain effect on the dielectric properties.

Based on this idea, we prepared two types of samples, with coherent and semi-coherent core/shell interfaces, by adding rare-earth elements (Dy, Ho, Er) of different ionic sizes. These rare-earth elements exhibit similar substitution behavior and similar effects on dielectric-temperature behavior[9,15] but have different effects on the residual strain.[16] Our experimental results show that the coherency strain at the core/shell interface considerably improves the dielectric-temperature stability of core/shell structured $BaTiO_3$ materials.

Samples with a composition of $92BaTiO_3$-$3R_2O_3$-3MgO-$2SiO_2$ (R: rare-earth) (mol %) were prepared from commercial powders of $BaTiO_3$ (0.3 μm, 99.99% purity, KCM Co., Nagoya, Japan), MgO (99.9% purity, Ube material industries, Ltd., Ube, Japan), SiO_2 (99.85% purity, Wako pure chemical industries, Ltd., Osaka, Japan), Dy_2O_3 (99.9% purity, Sigma-Aldrich Inc., MO, USA), Ho_2O_3 (99.9% purity, Sigma-Aldrich), and Er_2O_3 (99.9% purity, Sigma-Aldrich) powders. The proportioned powders were ball-milled, dried, sieved, and cold isostatically pressed at 200 MPa. After burning out the powder compacts at 900 °C for 1 h in air, the compacts were sintered at 1300–1350 °C in wet H_2 ($P_{O2} = 10^{-13} \sim 10^{-14}$ atm) for different periods of time. All the samples were densified to over 5.8 g/cm^3 during sintering. Microstructures were observed using a scanning electron microscope (Philips, Eindhoven, Netherlands) and a transmission electron microscope (JEOL Ltd., Tokyo, Japan) operated at 200 kV.

The crystal structures of the grains were identified, and the residual strain in the grains was estimated by the Hall-Williamson method[17,18] after conventional X-ray diffraction (XRD). The integral breadth at half-maximum intensity of the XRD peaks of five clear peaks (100, 101, 111, 200, and 202) was taken for estimation of the strain by profile fitting using MDI Jade 5.1 software. For the measurement of dielectric properties, the $BaTiO_3$ samples sintered in wet H_2 were re-oxidized at 1150 °C for 10 h in air. The dielectric properties were measured using an Agilent 4284A precision LCR meter with a 1 V_{rms} in a temperature range from −55 °C to 150 °C and a frequency range from 1 kHz to 1 MHz after coating an Ag paste on both surfaces of the samples. The

a)Electronic mail: sjkang@kaist.ac.kr

 © 2013 American Institute of Physics

This article is copyrighted as indicated in the article. Reuse of AIP content is subject to the terms at: http://scitation.aip.org/termsconditions. Downloaded to IP: 143.248.118.104 On: Thu, 11 Sep 2014 07:35:02

heating and cooling rate during the measurement was, respectively, 0.8 K/min.

Figure 1 shows TEM and SEM micrographs of (a) Dy-, (b) Ho-, and (c) Er-doped $BaTiO_3$ samples (hereafter, denoted as Dy-BT, Ho-BT, and Er-BT, respectively) sintered under different conditions. When co-doped with Mg, rare-earth containing $BaTiO_3$ commonly forms a core/shell structure during sintering.[9,16,19,20] The experimental conditions were chosen to obtain similar microstructures of the samples with different elements. The SEM micrographs in the insets of Figs. 1(a)–1(c) with typical core/shell grains show that the rare-earth doped samples have similar core and shell sizes. The bulk densities of different samples were also similar; the difference was less than 2%. Therefore, macroscopically, the samples have similar microstructures in terms of sintered density, grain size, and core/shell size.

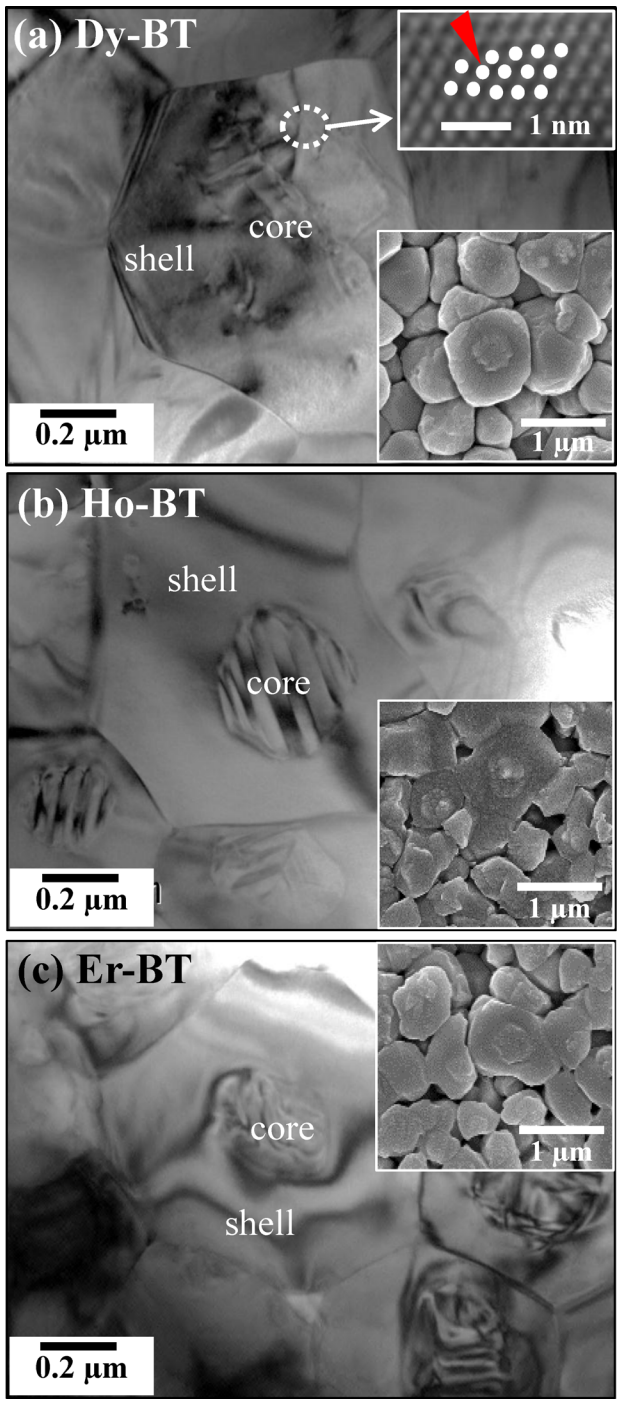

FIG. 1. TEM and SEM (insets) micrographs showing typical core/shell grains after sintering of (a) Dy-doped $BaTiO_3$ (Dy-BT) at 1300 °C for 30 min, (b) Ho-doped $BaTiO_3$ (Ho-BT) at 1350 °C for 1 h, and (c) Er-doped $BaTiO_3$ (Er-BT) at 1300 °C for 30 min. The upper inset in (a) is an inverse Fourier transformed HRTEM image showing an atomic mismatch near the core/shell interface.

Microscopically, however, there are substantial differences between Dy-BT, Ho-BT, and Er-BT, as the TEM micrographs in Fig. 1 show. The grains in Dy-BT contain many dislocations, in particular near the core/shell interface, while those in Ho-BT and Er-BT do not. One of the misfit dislocations in a grain of Dy-BT is magnified and shown in the upper inset of Fig. 1(a) as an inverse Fourier transformed image. An atomic mismatch near the core/shell boundary can clearly be seen.

The formation of misfit dislocations should result in loss of coherency strain, as in the case of coherency breaking with the formation of misfit dislocations during diffusion-induced grain boundary migration.[21–24] Figure 2 presents Hall-Williamson plots obtained from the XRDs of the three kinds of samples using the following equation (as the shapes of the diffraction peaks were mostly closer to Gaussian rather than Cauchy, the use of Eq. (1) is justified, unlike the case of a previous investigation.[25] In addition, regarding the strain states of different samples, plots obtained by using the equation for Cauchy shape gave the same conclusion as those obtained by using Eq. (1)):[17]

$$(\beta_{1/2}\cos\theta/\lambda)^2 = (0.89/d)^2 + 16\varepsilon^2(\sin\theta/\lambda)^2, \qquad (1)$$

where $\beta_{1/2}$ is the true integral breadth line at half maximum intensity after instrumental correction, d the grain size, and ε the elastic strain. In Fig. 2, the residual strain in the grains can be obtained from the slope of the plot. The values of $(\beta_{1/2}\cos\theta/\lambda)^2\times10^6$ and $(4\sin\theta/\lambda)^2$ are similar to those obtained in a previous study for $BaTiO_3$.[26] The slope of the Er-BT sample is the highest and that of the Dy-BT sample the lowest. The lowest slope of Dy-BT indicates that the strain in the core/shell grains is the lowest among different samples. In a previous investigation of rare-earth doped $BaTiO_3$, Park *et al.*[27] reported a similar low strain state of

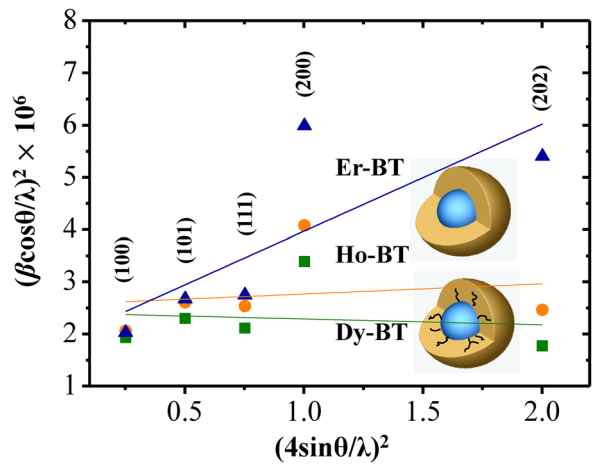

FIG. 2. Hall-Williamson plots for sintered Dy-BT, Ho-BT, and Er-BT samples.

This article is copyrighted as indicated in the article. Reuse of AIP content is subject to the terms at: http://scitation.aip.org/termsconditions. Downloaded to IP: 143.248.118.104 On: Thu, 11 Sep 2014 07:35:02

core/shell grains and additionally a reduction of residual strain with grain growth (shell thickening) in Dy-doped samples. They also observed, on the other hand, that the strain of Y-doped core/shell grains increased continuously without appreciable grain growth as the sintering temperature was increased. They suggested that the strain relaxation in the Dy-doped sample caused the grain growth. They did not, however, clarify the causes of the strain relaxation in the Dy-doped sample or the strain increase in the Y-doped sample with increasing sintering temperature.

Our results clearly show that the strain relaxation in Dy-BT is due to coherency breaking at the core/shell interface with the formation of misfit dislocations. In terms of mechanics, a core/shell structure is in a similar state to that of a hetero-epitaxial thin film. The shell phase with a lattice parameter different from that of the core should initially grow epitaxially on the core. At this stage, the residual strain in the shell is proportional to the degree of lattice mismatch between the core and the shell. When the coherency strain exceeds a critical value (ε_c), the coherency is broken with the formation of many misfit dislocations.[22,28]

The lattice parameter of the shell phase varies with the dopant species. Kishi *et al.*[16] measured the variation of the lattice parameter of $BaTiO_3$ for different rare-earth species and amounts in $BaTiO_3$-MgO-R_2O_3 systems (R: La, Sm, Dy, Ho, Er, and Yb). Among them, small rare-earth elements, Dy, Ho, and Er, are amphoteric with similar substitution behavior but result in significant differences in the lattice parameter. The lattice parameter of $BaTiO_3$ increased with addition of Er while it drastically decreased with addition of Dy and slightly decreased with addition of Ho (up to 3 mol %). Considering that the lattice volume of the core phase (pure $BaTiO_3$) expands (≈1%) with the cubic-tetragonal phase transition during cooling,[3] the lattice mismatch at the core/shell boundaries must be intensified with the substitution of a small rare-earth element, particularly Dy. The strain energy also increases with shell thickening accompanied by grain growth. When the residual strain energy exceeds a critical value with shell thickening, the strain energy is released with the introduction of many misfit dislocations at the core/shell interfaces, as in the case of thin film growth on a substrate.[28]

In our case, the Dy-BT sample should have the highest intensive residual strain ($>\varepsilon_c$) in the core/shell grains among the three kinds of samples although a slight increase of the ionic radius of Dy in the Ba-site is anticipated with the reduction from 3+ to 2+ at low temperature.[29,30] The strain in the Dy-BT sample appeared to be released with the formation of misfit dislocations near the core/shell interface, as shown in Fig. 1(a). On the other hand, the Er- and Ho-doped core/shell grains are thought to be under strains lower than a critical value as they maintained coherency at the core/shell boundaries.

Figure 3 plots the variation of the dielectric permittivity and tangent loss of the Dy-BT, Ho-BT, and Er-BT samples with temperature. The dielectric permittivity curve of Dy-BT shows a peak at 45 °C while Ho-BT and Er-BT present smooth curves, showing insensitive variation of the dielectric permittivity with temperature. This difference can also be quantitatively expressed as the degree of diffuseness in the modified Curie-Weiss law[31]

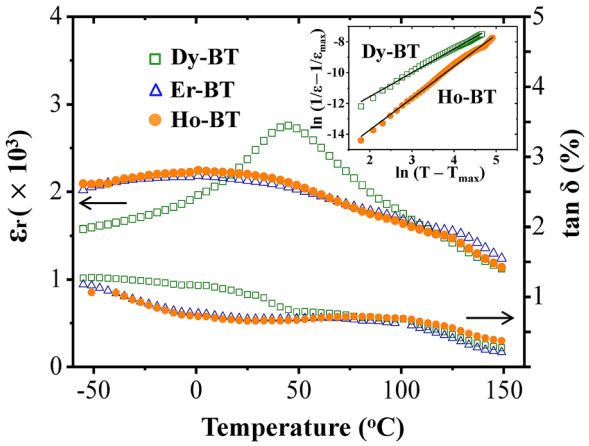

FIG. 3. Temperature dependences of dielectric permittivity and tangent loss at 1 kHz of Dy-BT, Ho-BT, and Er-BT samples in a temperature range from −55 to 150 °C. Plots of ln $(1/\varepsilon - 1/\varepsilon_{max})$ vs ln $(T - T_{max})$ for Dy-BT and Ho-BT are shown in the inset.

$$\frac{1}{\varepsilon} - \frac{1}{\varepsilon_m} = \frac{(T - T_m)^{\gamma}}{C}, \tag{2}$$

where ε_m is the maximum value of dielectric permittivity, ε is the dielectric permittivity at temperature T, T_m is the temperature at the peak of the dielectric permittivity, and C and γ are constants. The γ value represents the degree of diffuseness. γ has a value of 1 and 2 for a normal ferroelectric and for completely DPT, respectively.[32] From the plots of $\ln(1/\varepsilon - 1/\varepsilon_{max})$ vs $\ln(T - T_{max})$ in the inset of Fig. 3, the γ value was obtained as 1.54 for Dy-BT, ~2 for Ho-BT and Er-BT. The tangent loss of Dy-BT is similar to those of Ho-BT and Er-BT above T_m; however, below T_m, it is slightly higher than those of Ho-BT and Er-BT.

A similar temperature dependence of dielectric permittivity was also observed in Dy-, Y-, and Ho-doped $BaTiO_3$ samples by Park *et al.*[9] The Dy-doped core/shell structure showed peaked behavior while the Y- and Ho-doped core/shell structures showed typical broad curves, as in our study. As the grain size of the Dy-doped sample was larger than that of the other samples, they suggested that the distinct characteristics of the Dy-doped sample are related to the thickening of the shell. Our results, however, reveal that the inferior dielectric-temperature behavior of the Dy-BT sample is related to coherency breaking at the core/shell interface.

A considerable difference in the variation of the dielectric property with frequency was also observed among Ho-BT, Er-BT, and Dy-BT, as shown in Fig. 4. As the frequency increased, significant T_m shifts toward high temperature (frequency dispersion) were observed for Ho-BT and Er-BT (Fig. 4(a)): from 1 °C at 1 kHz to 15 °C at 1 MHz. In contrast, Dy-BT shows invariable T_m at 45 °C for the same frequency variation, as presented in Fig. 4(b). The frequency dispersion of Ho-BT can be described by the Vogel-Fulcher relationship[33,34]

$$f = f_0 \exp[-E_a/k_B(T_m - T_f)], \tag{3}$$

where f is the experimental frequency, f_0 is the pre-exponential factor, E_a is the activation energy for the relaxation process, k_B

This article is copyrighted as indicated in the article. Reuse of AIP content is subject to the terms at: http://scitation.aip.org/termsconditions. Downloaded to IP: 143.248.118.104 On: Thu, 11 Sep 2014 07:35:02

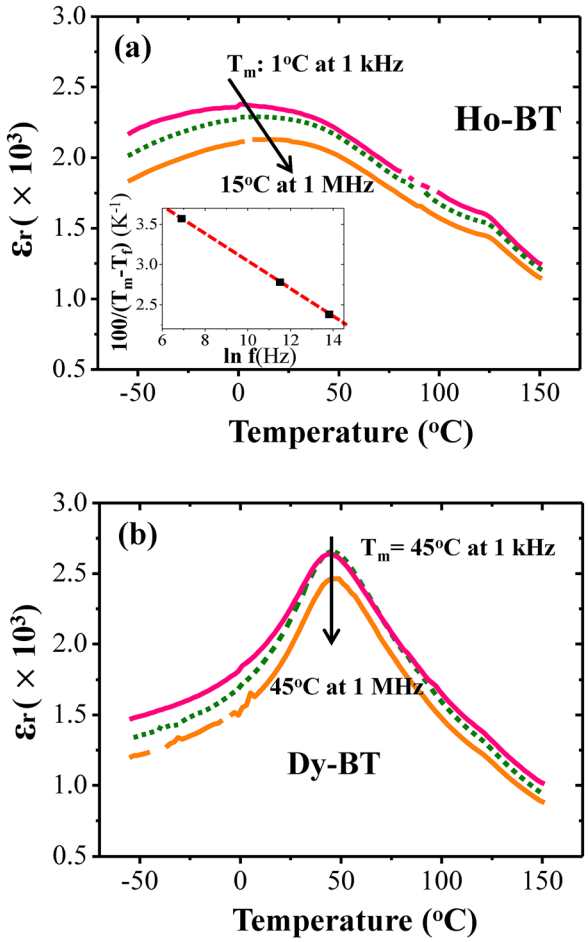

FIG. 4. Frequency and temperature dependences of the dielectric permittivity of (a) Ho-BT and (b) Dy-BT in a frequency range from 1 kHz to 1 MHz and a temperature range from −55 to 150 °C. The inset in Fig. 4(a) is a Vogel-Fulcher fit showing the frequency dependent T_m of Ho-BT.

is the Boltzmann constant, and T_m and T_f are the maximum temperature and freezing temperature in absolute value, respectively. The inset in Fig. 4(a) shows that the measured data fit the Vogel-Fulcher equation well. From the fitting, values of $f_0 = 9.81 \times 10^{11}$ Hz, $E_a = 0.05$ eV, and $T_f = 246$ K are obtained. These values are within the range of the calculated typical values for relaxor materials.[35,36] In addition, the merging of dielectric permittivity curves of Ho-BT (and Er-BT) for different frequencies at high temperature also indicates typical relaxor behavior, as usually observed in Pb-based relaxor materials.[37] Consequently, the frequency dispersion of T_m that is observed in Ho-BT and Er-BT is a typical characteristic of relaxor ferroelectrics showing DPT.[36–38] It can be therefore concluded that the residual strain (coherency strain) induced DPT, confirming the previous suggestion of an internal stress effect on DPT.[3]

Correa *et al.*[39,40] studied the residual strain effect in a $PbSc_{0.5}Nb_{0.25}Ta_{0.25}O_3$ system by comparing the dielectric-temperature behaviors of strain-induced thin film and strain-released bulk samples. They observed a strong frequency dispersion of T_m in the strain-induced thin films while frequency independent peak position was noted in the strain-released bulk samples. If the residual strain is sufficiently intensive to change the position of ions, frequency dispersion is an indication of the destruction of long range ordering of atoms by a residual strain.[40] The destruction of long range ordering leads to a local distortion of the crystal structure, giving rise to the formation of polar nano-regions (PNRs).[35,36] Our study shows that the difference in the observed frequency dependency between the Dy-BT sample and the Ho-BT and Er-BT samples is related, respectively, to the absence and the presence of coherency strain at the core/shell interface. The difference is also an indication of insignificant and significant presence of PNRs in the shell region.

The present microstructural observations and dielectric property measurements demonstrate that the coherency strain in core/shell grains has a significant contribution to temperature stability of the dielectric permittivity. The effect of the coherency strain on the formation of PNRs in the shell region, however, is not confirmed in the present investigation. More sophisticated TEM observations and micro-stress measurements are needed to identify the coherency strain effect on the formation of PNRs in the future.

In conclusion, the effect of coherency strain at the core/shell interface on the dielectric-temperature behavior of $BaTiO_3$ has been investigated with doping of three rare-earths (Dy, Ho, Er). Coherency between the core and shell was maintained in the Ho- and Er-doped $BaTiO_3$ samples while the coherency was broken with the formation of many misfit dislocations in the Dy-doped samples. The temperature stability of the dielectric properties was much better for the samples with a coherent interface than for the samples with a semi-coherent interface. The superior dielectric-temperature response in samples with a coherent interface is attributed to the coherency strain present in the core/shell grains, which can induce the formation of PNRs in the shell region. The present results demonstrate that maintaining coherency at the core/shell interface is necessary to ensure good temperature stability of core/shell grained $BaTiO_3$.

This work was supported by the Samsung Electro-Mechanics Co. Ltd. through the Center for Advanced MLCC-Manufacturing Processes and also by the National Research Foundation of Korea (NRF) grant funded by the Korea government (MEST) (No. 2012-0005707). Dr. Byung-Kwon Yoon is acknowledged for his contribution in dielectric measurement.

[1]M. Kahn, Ph.D. dissertaiton, Pennsylvania State University, University Park, PA, 1969.
[2]D. Hennings and G. Rosenstein, J. Am. Ceram. Soc. **67**(4), 249 (1984).
[3]T. R. Armstrong and R. C. Buchanan, J. Am. Ceram. Soc. **73**(5), 1268 (1990).
[4]H.-Y. Lu, J.-S. Bow, and W.-H. Deng, J. Am. Ceram. Soc. **73**(12), 3562 (1990).
[5]C. A. Randall, S. F. Wang, D. Laubscher, J. P. Dougherty, and W. Huebner, J. Mater. Res. **8**(4), 871 (1993).
[6]Y. Park and H. G. Kim, J. Am. Ceram. Soc. **80**(1), 106 (1997).
[7]J. Nishikawa, T. Hagiwara, K. Kobayashi, Y. Mizuno, and H. Kishi, Jpn. J. Appl. Phys. **46**, 6999 (2007).
[8]K. Yasukawa, M. Nishimura, Y. Nishihata, and J. i. Mizuki, J. Am. Ceram. Soc. **90**, 1107 (2007).
[9]K. J. Park, C. H. Kim, Y. J. Yoon, S. M. Song, Y. T. Kim, and K. H. Hur, J. Eur. Ceram. Soc. **29**, 1735 (2009).
[10]Z. Tian, X. Wang, H. Gong, T.-H. Song, K. H. Hur, and L. Li, J. Am. Ceram. Soc. **94**, 973 (2011).
[11]Y. Park and S. A. Song, J. Mater. Sci. **6**, 380 (1995).
[12]T. R. Armstrong, L. E. Morgens, A. K. Maurice, and R. C. Buchanan, J. Am. Ceram. Soc. **72**, 605 (1989).

This article is copyrighted as indicated in the article. Reuse of AIP content is subject to the terms at: http://scitation.aip.org/termsconditions. Downloaded to IP: 143.248.118.104 On: Thu, 11 Sep 2014 07:35:02

[13]K. J. Choi, M. Biegalski, Y. L. Li, A. Sharan, J. Schubert, R. Uecker, P. Reiche, Y. B. Chen, X. Q. Pan, V. Gopalan, L.-Q. Chen, D. G. Schlom, and C. B. Eom, Science **306**, 1005 (2004).
[14]A. HarringtonSophie, J. Zhai, S. Denev, V. Gopalan, H. Wang, Z. Bi, A. T. RedfernSimon, S.-H. Baek, C. W. Bark, C.-B. Eom, Q. Jia, M. E. Vickers, and J. L. MacManus-Driscoll, Nat. Nanotechnol. **6**, 491 (2011).
[15]Y. H. Song and Y. H. Han, Jpn. J. Appl. Phys., Part 1 **44**, 6143 (2005).
[16]H. Kishi, N. Kohzu, J. Sugino, H. Ohsato, Y. Iguchi, and T. Okuda, J. Eur. Ceram. Soc. **19**, 1043 (1999).
[17]B. D. Cullity and S. R. Stock, *Elements of X-ray Diffraction*, 3rd ed. (Prentice-Hall, Englewood Cliffs, NJ, 2001), pp. 400–401.
[18]G. K. Williamson and W. H. Hall, Acta Metall. **1**, 22 (1953).
[19]C. H. Kim, K. J. Park, Y. J. Yoon, M. H. Hong, J. O. Hong, and K. H. Hur, J. Eur. Ceram. Soc. **28**, 1213 (2008).
[20]S.-C. Jeon, C.-S. Lee, and S.-J. L. Kang, J. Am. Ceram. Soc. **95**, 2435 (2012).
[21]M. Hillert and G. R. Purdy, Acta Metall. **26**, 333 (1978).
[22]Y.-J. Baik and D. N. Yoon, Acta Metall. **35**, 2265 (1987).
[23]Y. W. Rhee, H. Y. Lee, and S. J. L. Kang, J. Eur. Ceram. Soc. **23**, 1667 (2003).
[24]S.-J. L. Kang, *Sintering: Densification, Grain Growth, and Microstructure* (Elsevier, Oxford, 2005), p. 112.
[25]J. Moon, T. Li, C. A. Randall, and J. H. Adair, J. Mater. Res. **12**, 189 (1997).
[26]R. Asiaie, W. Zhu, S. A. Akbar, and P. K. Dutta, Chem. Mater. **8**, 226 (1996).
[27]K. J. Park, C. H. Kim, Y. T. Kim, and K. H. Hur, J. Korean Ceram. Soc. **46**, 181 (2009).
[28]W. Nix, Metall. Trans. A **20**, 2217 (1989).
[29]Y. Tsur, T. D. Dunbar, and C. A. Randall, J. Electroceram. **7**, 25 (2001).
[30]T. D. Dunbar, W. L. Warren, B. A. Tuttle, C. A. Randall, and Y. Tsur, J. Phys. Chem. B **108**, 908 (2004).
[31]W. J. Merz, Phys. Rev. **91**, 513 (1953).
[32]K. Uchino and S. Nomura, Ferroelectrics **44**, 55 (1982).
[33]G. Fulcher, J. Am. Ceram. Soc. **8**, 339 (1925).
[34]A. K. Tagantsev, Phys. Rev. Lett. **72**, 1100 (1994).
[35]H. Du, W. Zhou, F. Luo, D. Zhu, S. Qu, and Z. Pei, J. Appl. Phys. **105**, 124104 (2009).
[36]L. Cui, Y.-D. Hou, S. Wang, C. Wang, and M.-K. Zhu, J. Appl. Phys. **107**, 054105 (2010).
[37]M. M. Kumar, K. Srinivas, and S. V. Suryanarayana, Appl. Phys. Lett. **76**, 1330 (2000).
[38]L. E. Cross, Ferroelectrics **76**, 241 (1987).
[39]M. Correa, A. Kumar, and R. S. Katiyar, Appl. Phys. Lett. **91**, 082905 (2007).
[40]M. Correa, A. Kumar, and R. S. Katiyar, J. Am. Ceram. Soc. **91**, 1788 (2008).

This article is copyrighted as indicated in the article. Reuse of AIP content is subject to the terms at: http://scitation.aip.org/termsconditions. Downloaded to IP: 143.248.118.104 On: Thu, 11 Sep 2014 07:35:02